Synthesis and Characterization of Processable Polyaniline Doped with Novel Dopant NaSIPA

Parveen Saini,[1] Rajesh Jalan,[2] S. K. Dhawan[1]

[1]*Polymeric and Soft Materials Section, National Physical Laboratory, New Delhi 110 012, India*
[2]*Reliance Industries Ltd., Reliance House, Ballard Estate, Mumbai 400 001, India*

Received 7 March 2007; accepted 14 November 2007
DOI 10.1002/app.27827
Published online 23 January 2008 in Wiley InterScience (www.interscience.wiley.com).

ABSTRACT: Aniline has been polymerized in the presence of a novel dopant sodio-5-sulfo-isophthallic acid (NaSIPA), via the chemical oxidative polymerization route. The thermal stability and processability of polyaniline prepared by indirect method (PD1) have been improved significantly (290°C) as compared to polyaniline doped with conventional inorganic dopants like HCl or H_2SO_4, without much loss of electronic conductivity (5.07 S/cm in PD1). This suggests its use for melt blending with engineering thermoplastics. However, polyaniline prepared by direct method (PD2) can be melt-blended only with conventional thermoplastics like polyethylene, polypropylene, polystyrene, etc. Low-temperature studies reveal the 1-D variable range hopping as a conduction mechanism for direct polymer (PD2), with parameters T_o and σ_o as 4112 K and 15.1 S/cm, respectively. However, for indirectly doped polymer (PD1) Arrhenius-type model, having parameters $|(E_F - E_C)|$ and σ_C as 0.04 eV and 28.4 S/cm, respectively, it suited well. The coherence length as found from XRD data was around 28.8 nm for PD1 and 25.2 nm for PD2. © 2008 Wiley Periodicals, Inc. J Appl Polym Sci 108: 1437–1446, 2008

Key words: polyaniline; variable range hopping (VRH) conduction mechanism; conducting polymers; UV–vis spectroscopy; XRD

INTRODUCTION

Since the discovery of conducting polymers in the year 1977, these synthetic metals have become the core of the material science because of their novel electronic and electrical properties. These materials have broad application range covering energy storage,[1,2] sensors,[3–5] anticorrosive materials,[6–8] electromagnetic interference shielding,[9–11] electrostatic charge dissipation,[12–14] organic light emitting diodes,[15–18] plastic solar cells,[19,20] and supporting material for catalysis.[21,22] However, among other conducting polymers, polyaniline has been extensively studied, not only because its electronic conductivity can easily be tuned by adjusting the oxidation state and degree of doping of the backbone, but also due to its environmental stability as well as economic feasibility. Therefore, polyaniline is a promising futuristic material for various technocommercial applications.

Polyaniline polymerization proceeds by a conventional free radical mechanism[23–25] involving initiation, propagation, and termination steps. Chemically, polyaniline is made up of 50% reduced B—NH—B—NH and 50% oxidized B—N=Q=N— repeating units, where B denotes a benzenoid and Q denotes a quinoid unit. Thus, different ratios of these fully reduced and fully oxidized units yield various forms of polyaniline, such as leucoemeraldine (100% reduced form), emeraldine base (50% oxidized form), and pernigraniline (fully oxidized form). However, all of these forms are electrically insulating in nature. Doping of emeraldine base with a protonic acid converts it into conducting form protonated emeraldine (emeraldine salt). The doping of polyaniline leads to the protonation of imine nitrogen atoms, which results in the formation of bipolarons. These bipolarons are then converted into polarons via an internal redox reaction. Finally, the separation of polarons leads to the formation of highly delocalized polaron lattice,[26] imparting conductivity to the polymer.

Despite having a number of merits, the main issue associated with polyaniline is processing difficulties because of its infusibility and relative insolubility in common organic solvents. It can be made processable/soluble either by polymerizing functionalized anilines[27,28] or by copolymerizing aniline with substituted monomers.[29–31] Bulky counterion-induced processability[32,33] has also been reported by several groups. Electronic properties of these synthetic metals can be tailored by carrying out the polymerization under the controlled conditions and in the presence of specific dopants.

Polyaniline has been polymerized by a typical free radical mechanism.[23] Initiation was effected by

Correspondence to: S. K. Dhawan (skdhawan@mail.nplindia.ernet.in).
Contract grant sponsor: Reliance Industries Ltd., India.

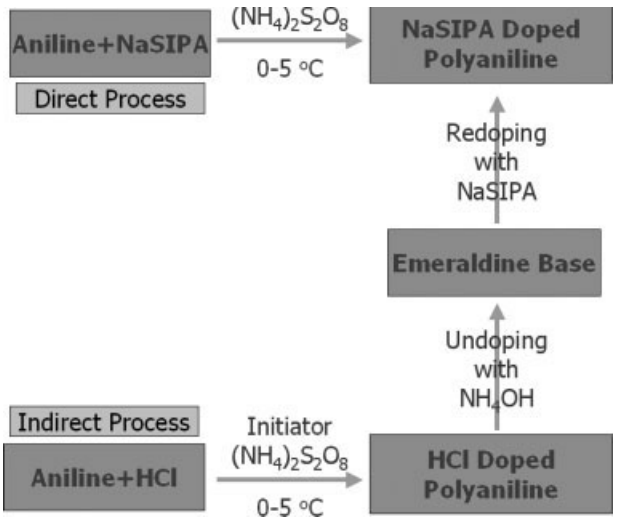

Scheme 1

$(NH_4)_2S_2O_8$ (APS), which under the proper pH conditions form the primary radicals that react with aniline monomer to form radical cations that can be represented by various canonical forms.[24] Propagation step involves the addition of radical cations to oligomeric species to form polymeric chains. Because of the steric hindrance offered by the $—NH_2$ group, ortho coupling has almost been excluded leading to the formation of a para product. However, some ortho coupling[25] also occur leading to the formation of corrupted polymer. Chain growth continued till it is terminated either by chain transfer or by coupling of radicals. Low temperature favors the formation of long chains (high molecular weights).

In the present article, we report the use of sodio-5-sulfo-isophthallic acid (NaSIPA) as bulky counter ion to improve processability of polyaniline. The polymerization was carried out via the chemical oxidative polymerization route. The doping was carried out through both direct and indirect approach as shown in Scheme 1. The polymers so synthesized were characterized by the various techniques like thermogravimetric analysis (TGA), differential scanning calorimetry (DSC), FTIR, UV–visible spectroscopy, XRD, etc. Their electronic conductivities were measured by four-probe technique. Variable range hopping (VRH) and Arrhenius models have been applied depending upon the nature of variation of conductivity with temperature.

The solubility and thermal stability of the polyaniline direct doped with NaSIPA (PD2) has been found to be significantly higher than polyaniline doped with small dopants like HCl. However, their electronic conductivities are substantially lower than latter. To maintain balance between conductivity, stability, and processability indirect doping approach has been used. The higher thermal stability and acceptable electronic conductivity makes these polymers a potential candidate for melt blending with engineering thermoplastics like polyamides, polyester, polycarbonate, etc.

EXPERIMENTAL

Materials

Aniline (Loba Chemie, India), HCl (35.4% SD Fine-Chem, India), NaSIPA (Eastman Chemical Company, India), and ammonium persulfate (APS, Merck, India) were used without further purification. Liq. NH_3 (30%, Loba Chemie, India) was used to dedope the doped polymers. *N*-Methyl pyrrolidone (NMP, Merck), *N*,*N*-dimethyl formamide (DMF, Qualigens, India), and acetone (Merck) were used for making solutions. Monoethylene glycol (MEG, Qualigens, India) used was of AR grade. Aqueous solutions were prepared from the double distilled water, having a specific resistivity of 1 MΩ cm.

Polymer preparation

As discussed in Introduction, the doped polyaniline was prepared by free-radical chemical oxidative polymerization, through both direct and indirect routes.

Direct approach

For the direct route, 0.1 mol of aniline and 0.5 mol of NaSIPA were mixed in 1.0 L of water. Polymerization was initiated by the drop wise addition of ammonium persulfate (0.1 mol in 100 mL distilled water). The polymerization was carried out at a temperature of $-5.0°C \pm 1.0$ °C and over a period of 4–6 h. The polymer has been produced directly in the doped state as a dark green precipitate, dispersed in the reaction mixture. The aforementioned mixture was filtered, and the precipitate so obtained was washed repeatedly with distilled water till the pH of the filtrate became neutral. The final precipitate was then dried under dynamic vacuum till constant weight. The dried mass was then crushed to obtain the powder of the doped polymer (PD2). The earlier-synthesized powder (PD2) was then treated with 1.0*M* aqueous ammonia and stirred for 2 h to convert it to the base/undoped form (PB2). The PB2 powder was then obtained by the processes of filtration, rinsing, and drying successively.

Indirect approach

For the indirect route, 0.1 mol of aniline and 0.5 mol of HCl were mixed in 1.0 L of water. The polymerization was carried out using APS (0.1 mol in 100 mL distilled water) as initiator and for the same duration and conditions as in the case of direct approach. The doped polymer powder so obtained was then treated with 1.0*M* aqueous ammonia to obtain the base form of polyaniline (PB1). The PB1 was then treated with

TABLE I
Characteristics of Polyaniline Prepared by Direct and Indirect Routes

	Base form of the PANI (polymerized in the presence of HCl medium)(PB1)	Base form of the PANI (polymerized in the presence of NaSIPA medium) (PB2)	NaSIPA doped PB1 (indirect approach) (PD1)	PANI polymerized in the presence of NaSIPA medium (direct approach) (PD2)
COO^- group of dopant	–	–	1693	1698
N-Quinoid	1582	1584	1556	1559
N-Benzenoid	1494	1495	1483	1489
C—N stretching	1308	1288	1294	1286
C—H in-plane bending	1160	1164	1101	1105
Stretching of SO_3^- of dopant	–	–	1032	1036
C—H out-of-plane bending	825	824	794	802
1,3,5-Trisubstituted benzene ring of dopant	–	–	752	753
Bending modes of SO_3^- of dopant	–	–	667, 616	671, 615

0.5*M* aqueous NaSIPA solution and stirred for 2 h to obtain the doped form of the same polyaniline (PD1). The PD1 powder was again obtained by filtration and drying.

The earlier-synthesized polymers were designated on the basis of doping approach (i.e., direct or indirect) and their detailed descriptions along with the abbreviations have been presented in Table I.

Measurements

For the conductivity measurements, pellets of dimensions of length 13 mm, width 7 mm, and thickness 1–2 mm were prepared, and the resistivities were measured by four-point probe technique using Keithley 220 Programmable Current Source and 181 Nanovoltmeter. Mettler Toledo TGA/SDTA 851[e] and Mettler Toledo DSC 822[e] were used to observe the thermal behavior. Materials were heated from 25 to 700°C under a constant heating rate of 10°C/min, in the inert atmosphere of nitrogen. The samples were also studied by using Shimadzu UV-1601 UV–visible spectrophotometer after preparing solutions of their base forms in NMP, and DMF and doped forms in MEG. NICOLET 5700 FTIR spectrometer and D8 Advance Bruker AXS X-ray diffractometer (Cu Kα 1.54098 Å as source) were used to observe the characteristic peaks of these polymers.

RESULTS AND DISCUSSION

Conductivity

Figure 1 shows the relationship between voltage and current in the doped polymers PD1 and PD2 at room temperature. The voltage increases linearly with the

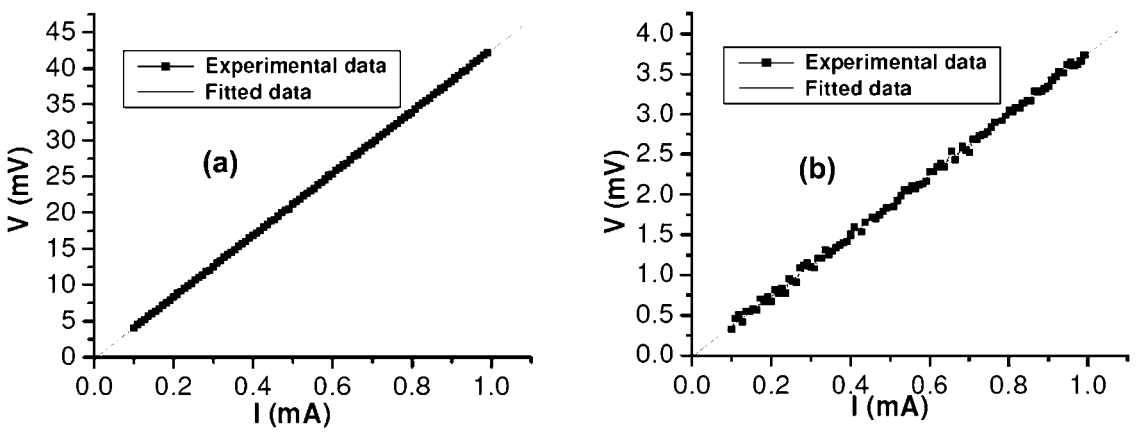

Figure 1 Relationship between current and voltage for doped polymers (a) PD2 and (b) PD1 at room temperature.

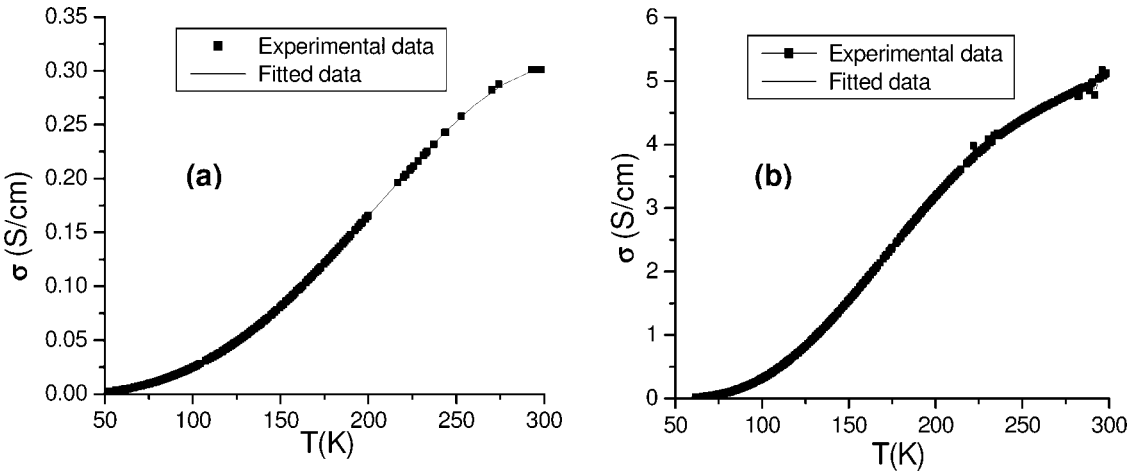

Figure 2 Plots of d.c. conductivities (σ) versus temperature (T) for doped polymers (a) PD2 and (b) PD1 at room temperature.

increasing current, indicating that the polymers represent ohmic behavior. The slope of the straight line between voltage–current plots gives the resistance ''R'' of the samples, which ultimately gives the conductivity by taking into account dimensions of the samples.

The conductivity σ of the pellet is given by the following relation:

$$\sigma = \frac{l}{RA}$$

where ''l'' is the length of the pellet, ''R'' is resistance, and ''A'' is the cross-sectional area of the pellet.

The room temperature resistance values of doped PD2 and PD1, as evaluated from slopes of Figure 1 (curves a and b) are 42.7 and 3.77 Ω, respectively. Taking into account the dimensions of pellets, the corresponding values of conductivities are found to be 0.298 and 5.07 S/cm, respectively.

Figure 2 shows the variation of conductivities of PD1 and PD2 with temperatures in the range of 50–300 K. As can be viewed, conductivity of both the samples increases exponentially with the temperature. This shows that these polymers obey temperature dependence of conductivity similar to conventional semiconductors.

We have also tried to fit the appropriate model for the variation of conductivity of the materials with temperature. For the aforementioned models, we have studied the response of samples in both VRH[34–37] and Arrhenius type transport[38] regimes. In the VRH regime, temperature dependence of conductivity σ follows the generalized relation:

$$\sigma = \sigma_o \exp\left[-\left(\frac{T_o}{T}\right)^{1/r}\right]$$

where T_o is the Mott characteristic temperature and is a measure of the hopping barrier and σ_o is conductivity at infinite temperature. Their values are determined by density of states, localization length, and average hopping distance. The value of ''r'' is related to the dimensionality (d) of the system as $r = (d + 1)$. For the one-, two- and three-dimensional systems, ''r'' is equal to 2, 3, and 4, respectively.

In the Arrhenius-type transport, temperature dependence of conductivity σ follows the generalized relation:

$$\sigma = \sigma_C \exp\left[-\frac{|(E_F - E_C)|}{kT}\right]$$

where $(E_F - E_C)$ is the energy difference between the Fermi energy and mobility edge and σ_C is the conductivity at the mobility edge.[39]

Figure 3 shows the variation of conductivities for both PD1 and PD2 when plotted as ln σ versus $T^{-1/2}$, $T^{-1/3}$, $T^{-1/4}$, and T^{-1}, respectively. These plots have been fitted for linear correlations. The quality of linear fit is represented in terms of fit factor (FF) and standard deviation (SD). For the good fitting, FF should be as close as possible to unity, whereas SD should approach zero.

As can be seen from Figure 3 (curves a, c, e and g) for the direct-doped sample (PD2), linear dependence of the ln σ on $T^{-1/2}$ is better than that on either of $T^{-1/3}$, $T^{-1/4}$, or T^{-1}. The former has a linearity FF of 0.99967 and shows SD of only 0.03832. Thus, 1D-VRH ($r = 1$) model suits better for PD2. Therefore, for PD2 the values of T_o and σ_o as evaluated from the slope of the straight line of the Figure 4(c) are 4112 K and 15.1 S/cm, respectively. On the other hand, Figure 3 (curves b, d, f, and h) reveals that, for the PD1, linear dependence of the ln σ on T^{-1} is better than either on $T^{-1/2}$, $T^{-1/3}$, or $T^{-1/4}$ and the linearity FF and SD for the same are found to be 0.99789 and 0.09762, respectively. Therefore, Arrhenius-type transport seems to be an appropriate choice for the PD1. This suggests the existence of band-type conduction, and the values of $(E_F - E_C)$ and σ_C as obtained from straight line of

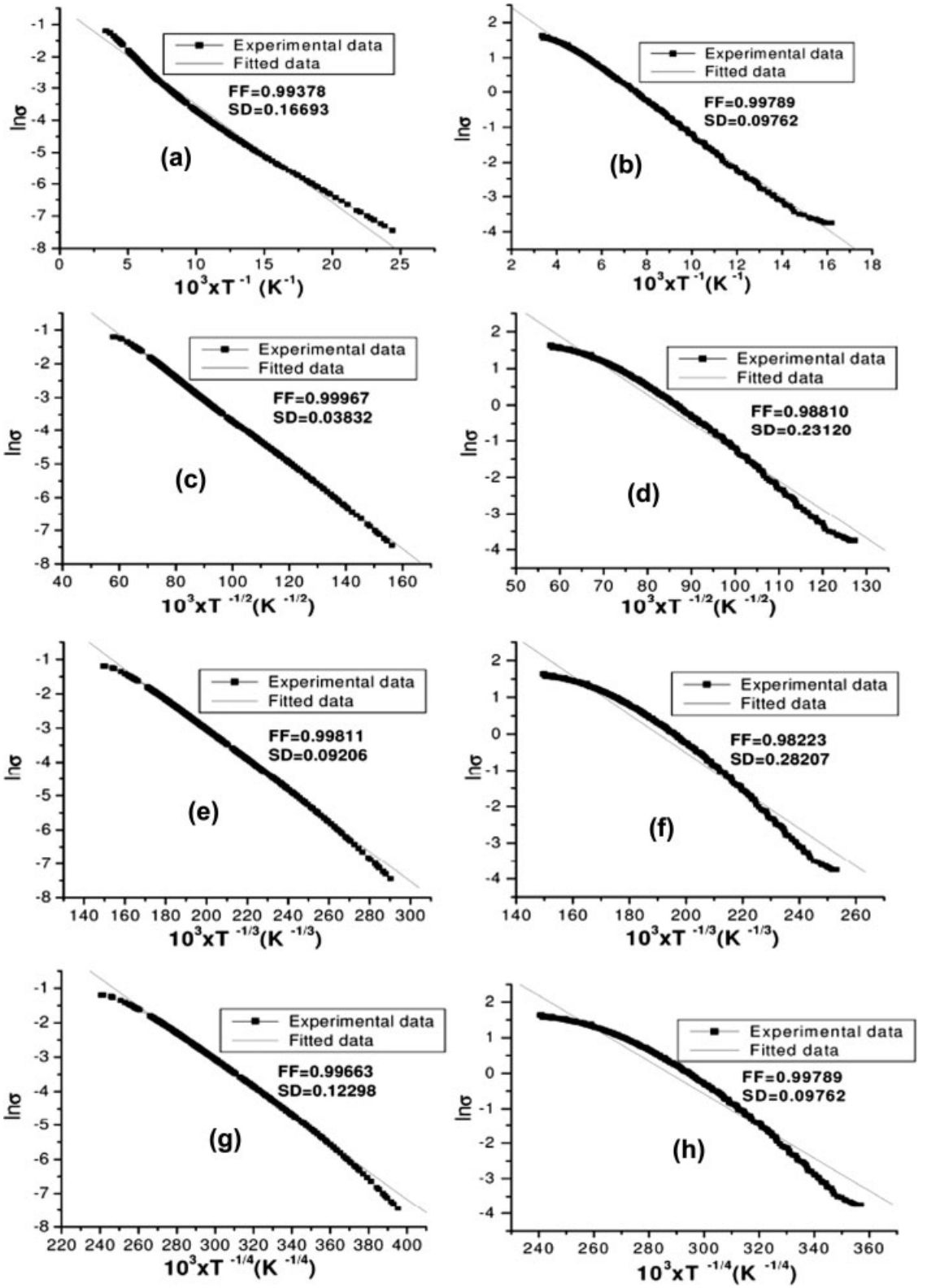

Figure 3 Plots of ln σ versus T^{-1}, $T^{-1/2}$, $T^{-1/3}$, and $T^{-1/4}$ for doped polymers curves (a), (c), (e), (g) for PD2 and curves (b), (d), (f), (h) for PD1.

Figure 3(b) are found to be 0.04 eV and 28.4 S/cm, respectively.

The conductivity data shows that direct-doped samples are less conducting than indirectly doped polymers. The conductivity decreases both due to decrease in conjugation length as well as less doping level achieved. Further, the higher amount of NaSIPA (which is an insulating material) in PD2 than in PD1

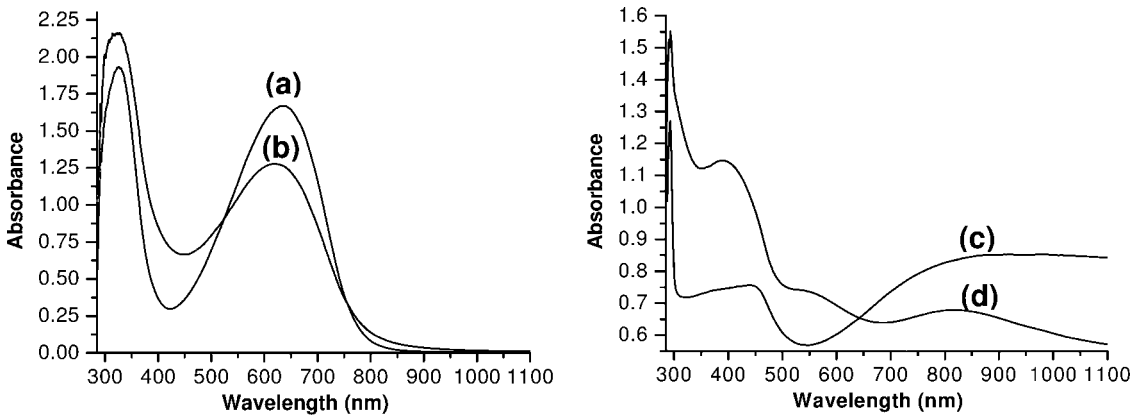

Figure 4 UV–visible absorption spectra of base forms in NMP curves (a) PB1 and (b) PB2 and doped forms in MEG curves (c) PD1 and (d) PD2.

leads to partial blockage of the conduction path and subsequently reduces the conductivity.

UV–visible absorption spectra

Figure 4 (curves a and b) shows UV–visible absorption spectra of base forms PB1 and PB2, respectively, in NMP solvent. For base forms, there are two peaks in the UV–visible range, one around 320 nm is due to the π->π* transition (band-gap) and is directly related to the extent of conjugation. The other peak 630 nm is due to the molecular exciton associated with the quinine–diimine structure[40] i.e., transition between HOMO orbitals of benzenoid rings and LUMO orbitals of the quinoid rings.

The UV–visible data reveals that π->π* band in PB2 shifts to the lower wavelength (hypsochromic shift) w.r.t. the PB1 which can be attributed to the dopant-induced alteration of the torsional angle, and subsequent reduction of conjugation length. The degree of hypsochromic shift in PB2 is directly related to the reduction in conjugation lengths w.r.t. PB1. Therefore, the PB1 absorbs at 329 nm in NMP, whereas PB2 gives a band around 323 nm.

Also the higher relative intensity of 320 nm w.r.t. 630 nm band in case of PB2 than in PB1 reveals that PB2 is present in much more reduced state than PB1. Thus, PB2 has more benzenoid rings than quinoid, whereas in case of PB1 they are present in almost equal proportions.

Now more benzenoid content of PB2 suggests its absorption around 320 nm should be higher than that of PB1 (329 nm). However, the lower conjugation length favors the absorption at lower wavelength than PB1. Thus, there are two competing factors and lower absorption wavelength of PB2 than PB1, suggesting that a decrease in conjugation dominates over the higher benzenoid content factor. However, both the aforementioned factors leads to both lower electronic conductivity as well as thermal stability.

Figure 4 (curves c and d) shows the UV–visible spectra of the doped samples (PD1 and PD2), respectively, in MEG. The spectra show that bands of PD1 are located at 293, 365, 428, and 910 nm, respectively, whereas those of PD2 are at 293, 390, and 810 nm. The band around 360 nm is due to the π->π* transition, whereas bands around 430 nm (polaron->π*) and 850 nm (π->polaron).[41] are the characteristics of localized polaronic states and indicate the presence of polymers in their doped forms in MEG solvent.

The presence of much better developed π->polaron band in PD1, having a tail deep into NIR suggests that polarons in PD1 are more delocalized than in case of PD2. The UV data also reveals that, in case of PD2, the band around 360 and 430 are merged to give a single band around 390 nm. The presence of a weak shoulder around 565 nm (reminiscence of undoped form) in case of PD2 suggests relatively less degree of doping. To confirm the same, we have compared the relative intensities of the bands around 810–910 nm w.r.t. 290- to 300-nm band. The higher value in case of PD1 suggests that the same has much higher achieved doping levels than that of PD2.

FTIR spectra

The characteristic FTIR bands of the base (PB1 and PB2) and doped (PD1 and PD2) forms of the polymers have been recorded in the Table I. In the base forms, the intensity ratio of 1580 and 1490 cm^{-1} band could be used to determine the oxidation state of the material.[42] This ratio was 0.953 for PB1 and 0.707 for PB2. This suggests that PB1 has equal number of benzenoid (0.51) and quinoid (0.49) units, and thus has a nearly pure emeraldine-type structure. However, the comparatively smaller ratio for PB2 suggests the presence of more benzenoid (0.60) than quinoid (0.40) units. Thus, PB2 may be present in a slightly reduced state. The comparatively reduced structure of the PB2

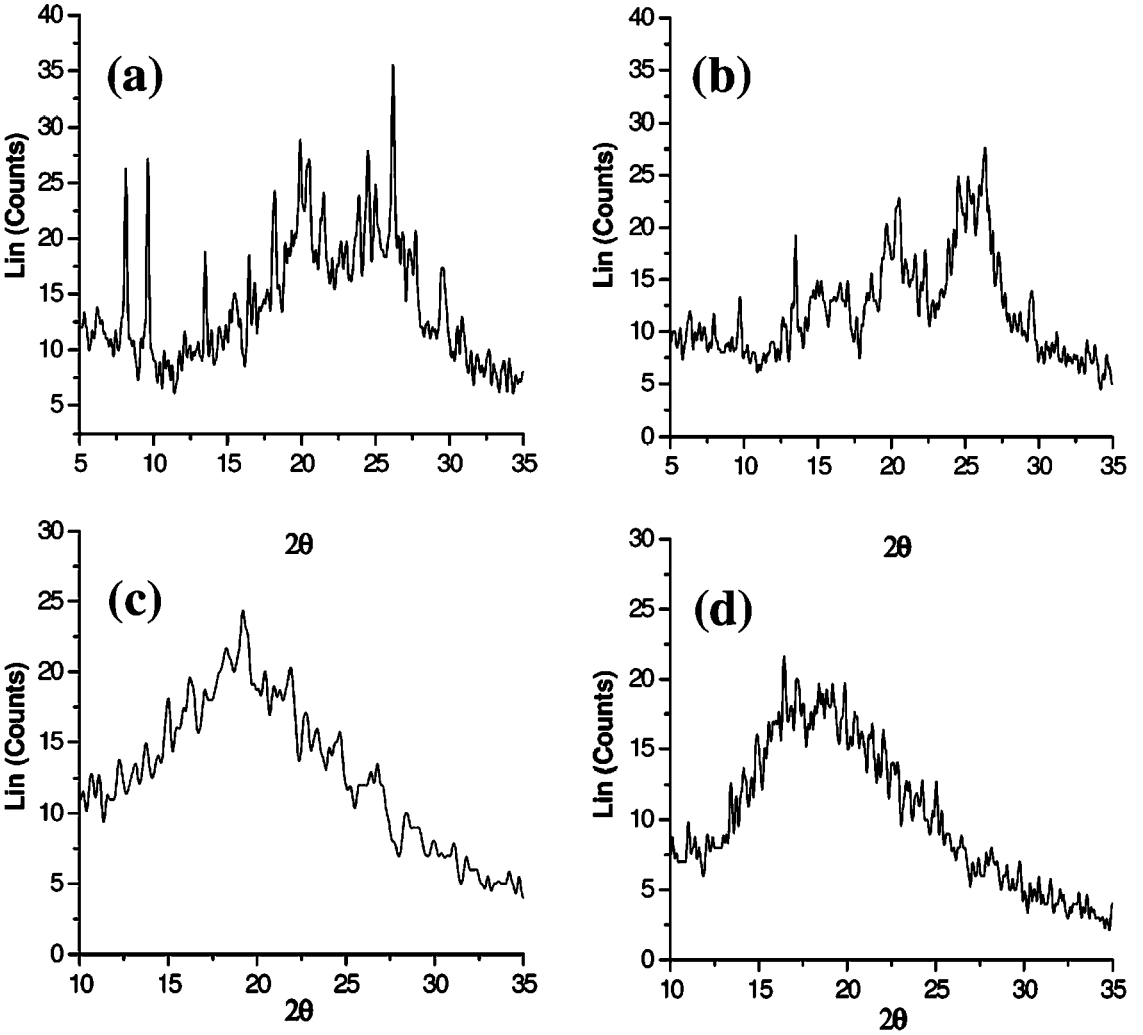

Figure 5 XRD patterns of the polymers (a) PD2, (b) PD1, (c) PB2, and (d) PB1.

has also been complemented by the UV–visible data of the materials.

The characteristic FTIR bands of dopant (NaSIPA) are located at 1712 and 1736 cm^{-1} (—COOH stretching), 1120 (C—H in-plane bending), 1042 (—SO_3 stretching), and 600–700 cm^{-1} (—SO_3 deformation). On doping the base, the band intensity of 1400 and 1500 cm^{-1} bands decrease significantly (because of the internal redox reaction and formation of polaronic lattice), and a sharp intense band appears around 1100 cm^{-1}. This free carrier band around 1100 cm^{-1} is much broader and intense in case of PD1 than in PD2, which indicates more charge delocalization in former. In case of doped samples (Table I), all the major bands of dopant NaSIPA are present but the relative intensity of these bands is more in PD2 than in PB1, thus indicating more NaSIPA content of the PD2. The same has also been conferred by XRD, where main peaks of NaSIPA are more intense in PD2 than in PD1. This extra/stray dopant leads to lower conductivity of PD2 than PD1.

XRD studies

Figure 5 (curves c and d) shows the X-ray diffraction pattern of the powdered samples PB2 and PB1, respectively. The pattern shows a broad halo centered on the 2θ value of 20°. The presence of halo indicates that the base form is amorphous. However, a pattern of PB2 exhibits a relatively sharp halo around 2θ = 19.5°. This may be related to the dopant-induced change in the supermolecular structure of the polymer. The main diffraction peaks of PD2 (curve 5a) are situated at 2θ values of 9.6 (d = 9.18 Å), 13.5 (d = 6.55 Å), 19.9 (d = 4.46 Å), 20.5 (d = 4.32 Å), 24.5 (d = 3.63 Å), 25.0 (d = 3.56 Å), 26.2 (d = 3.40 Å), and 29.6 (d = 3.02 Å), whereas that of PD1 (curve 5b) are located at 2θ value of 9.7 (d = 9.10 Å), 13.5 (d = 6.55 Å), 19.7 (d = 4.5 Å), 20.5 (d = 4.32 Å), 24.5 (d = 3.62 Å), 25.2 (d = 3.53 Å), 26.4 (d = 3.38 Å), and 29.5 (d = 3.03 Å. Among these, peaks around 2θ values of 9.7, 19.7, and 26.4 are characteristic peaks of dopant. However, peaks around 2θ values of 20.5 and 25.2 are character-

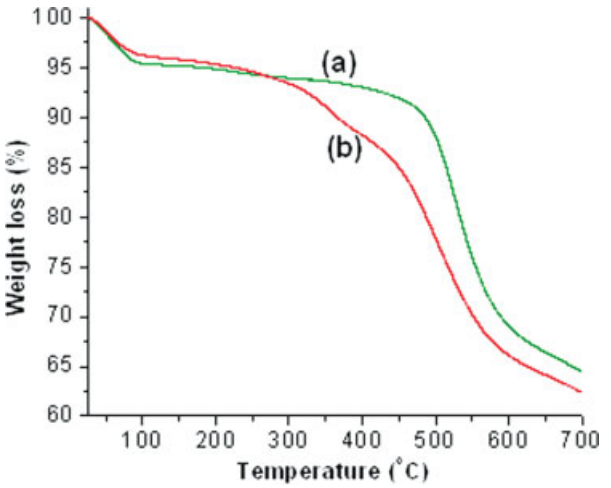

Figure 6 TGA graphs of base forms of polymers (a) PB1 and (b) PB2. [Color figure can be viewed in the online issue, which is available at www.interscience.wiley.com.]

istic of doped emeraldine salt form of polyaniline and are related to the periodicity parallel and perpendicular to the polymeric chains.[43,44] The aforementioned data reveals that the doped polymers PD1 and PD2 are partially crystalline relative to the respective undoped (base) forms.

Furthermore, peaks of pure dopant NaSIPA were more pronounced and sharper in the XRD pattern of PD2 than in PD1. This indicates more NaSIPA content in the polymer synthesized by direct method (PD2) than that of polymer prepared by indirect method (PD1). The same has also been indicated by the FTIR spectra of the samples. Also the peak around 2θ values of 25° is much well developed in case of PD1 than that of PD2, indicating that doping levels achieved are higher in PD1 than in PD2. This fact was also complemented by the UV–visible and FTIR data.

The crystallite size/coherence lengths of the crystalline domains of the PANI-NaSIPA and pure NaSIPA can be estimated from the X-ray peak broadening of the diffraction peaks, using Scherrer formula.[45] The coherence length for PD1 from 25° peak is 28.8 nm, whereas that of PD2 is 25.2 nm. Thus, the crystalline domain size is more in PD1 than in PD2, indicating more charge delocalization in the former.

Thermogravimetric analysis

Figure 6 (curves a and b) shows the TGA of the PB1 and PB2, respectively, revealing that both polymers have almost same stability up to 270°C. However afterwards, curves diverge and PB2 shows significant loss up to 400°C. On the other hand, PB1 shows good stability up to 430°C. The data clearly reveal that the thermal stability of PB2 is less than PB1. The onset of loss around 270°C reflects the reminiscence of leucoemeraldine state. Thus, low stability of PB2 may be attributed to the decreased conjugation length and molecular weights as well as lower oxidation state than PB1. After 430°C, both the polymers show a sharp weight loss, which can be correlated with the loss of the polymeric backbone and continued even after 700°C.

Figure 7 (curves a–c) shows the thermal stabilities of the dopant NaSIPA, PD1, and PD2, respectively. From the TGA data it is quite clear that all the samples show five noticeable weight loss steps. The relative positions of onset and endset temperatures of the loss steps vary from one sample to another depending on the material characteristics. The first weight loss is due to bound and free water. The sharp weight loss is from 440 to 490°C in case of dopant NaSIPA, where it suddenly loses 32% due to the onset of degradation and subsequent removal of CO_2. As evident from the first loss step, the free moisture content of the doped polymers was ~6%. During the second loss step, both PD1 (95–170°C) and PD2 (105–150°C) show almost similar thermal profiles. The third loss step for PD1 (170–280°C) and PD2 (150–230°C) may be linked to the condensation reaction between the —NH— groups of polymeric backbone and —COOH groups of dopant molecules. The fourth and fifth steps correspond to the further degradation of the materials. From the TGA data, it is quite clear that PD1 has good thermal stability even in the vicinity of 290°C, whereas PD2 is stable only up to 230°C. This envisages PD2 as a good candidate for melt blending with only conventional thermoplastics (polyethylene, polypropylene, polystyrene, etc.), but PD1 could also be melt-blended with engineering thermoplastics like polyamides, polyester, polycarbonates, etc.

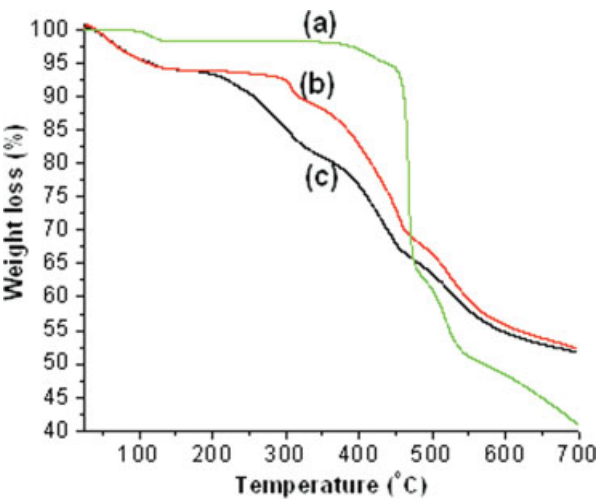

Figure 7 TGA graphs (a) dopant NaSIPA and doped forms of polymer curves (b) PD1 and (c) PD2. [Color figure can be viewed in the online issue, which is available at www.interscience.wiley.com.]

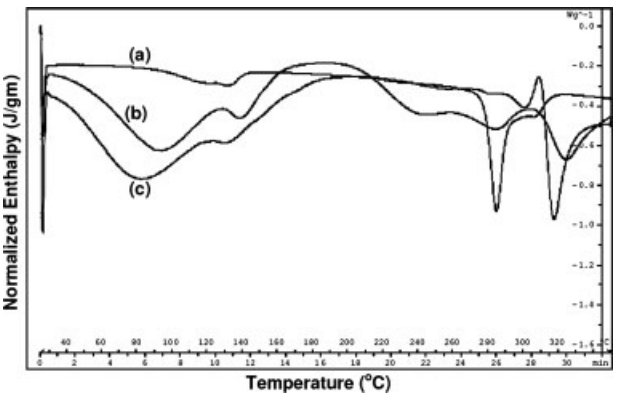

Figure 8 DSC graphs of (a) dopant NaSIPA and doped forms of polymer curves (b) PD2 and (c) PD1 in nitrogen at 10°C/min.

Differential scanning calorimetry

Figure 8 (curves a–c) shows the DSC plots of the NaSIPA, PD2, and PD1, respectively. The pure NaSIPA shows a broad transition centered around 140°C and a sharp transition around 280°C and a weak broad shoulder at 320°C, with no clear distinction between the last two steps. The posterior melting transition at 280°C is due to the disordered phase of dopant moiety. The 320°C is the melting point of the dopant.

The DSC plot of PD1 shows a broad endothermic peak centered on 95°C and having a weak shoulder around 130°C. However, in case of PD2, the peak is centered on 105°C, and a sharper shoulder was placed around 140°C. The broad peak is due to the moisture content of the material and shoulder may be attributed to some the changes related to the dopant. The smaller normalized area of the broad peak in case of PD2 than in PD1 and a sharper shoulder in case of the former indicates higher free NaSIPA content of the PD2 than PD1.

CONCLUSIONS

Conducting polymers of polyaniline doped by novel dopant NaSIPA have been prepared both by direct and indirect approaches. The direct-doped polymer has been significantly lower in conductivity and thermal stability than indirect-doped polymer. Therefore, indirect polymer has been focused in the present article.

UV and FTIR data revealed that PD2 is formed in more reduced state and has lower conjugation length than PD1. Also as revealed by UV and XRD data, the doping levels are much higher in case of PD1. The room temperature conductivity of PD1 has been found to be an order of magnitude higher than PD2. XRD and FTIR data also revealed that the free NaSIPA content of the PD2 is higher than PD1.

The low-temperature conductivity plots suggest that 1-D VRH is proper model for PD2, whereas for PD1 Arrhenius-type transport mechanism seems to be an apt choice. Room temperature conductivities of PD1 and PD2 were found to be 5.07 and 0.298 S/cm, respectively. The coherence length as found from XRD was around 28.8 nm for PD1 and 25.2 nm for PD2.

The thermal data suggests that PD1 has higher thermal stability than PD2 and can be used for melt blending with engineering thermoplastics.

Authors thank Dr. Vikram Kumar for his keen interest in the work and for giving permission to publish the results. Thanks are also to Dr. Harikishan and Sh. K.P. Singh for doing resistivity measurements of conducting polymer samples. We are highly obliged to Mr. K. N Sood and Dr. Ram Kishore for recording the SEM data and Dr. S. K. Halder, Dr. R. P. Pant, and Mr. Vinod for XRD patterns.

References

1. Kitani, A.; Kaya, M.; Saski, K. J Electrochem Soc 1995, 133, 1069.
2. Kumar, G.; Sivashanmugam, A.; Muniyandi, N.; Dhawan, S. K.; Trivedi, D. C. Synth Met 1996, 80, 279.
3. Scorsone, E.; Christie, S.; Persaud, K. C.; Kvasnik, F. Sens Actuators B 2004, 97, 174.
4. Koul, S.; Chandra, R.; Dhawan, S. K. Sens Actuators B 2000, 75, 151.
5. Aussawasathien, D.; Dong, J.-H.; Dai, L. Synth Met 2005, 154, 37.
6. Dhawan, S. K.; Trivedi, D. C. Synth Met 1993, 60, 67.
7. Qgurtsov, N. A.; Pud, A. A.; Kamarchik, P.; Shapoval, G. S. Synth Met 2004, 143, 43.
8. Jeyaprabha, C.; Sathiyanarayanan, S.; Venkatachari, G. J Appl Polym Sci 2006, 101, 2144.
9. Dhawan, S. K.; Singh, N.; Venkatachalam, S. Synth Met 2002, 129, 261.
10. Dhawan, S. K.; Singh, N.; Rodrigues, D. J Sci Technol Adv Mater 2003, 4, 105.
11. Yavuz, Ö.; Ram, M. K.; Aldissi, M.; Poddar, P.; Srikanth, H. Synth Met 2005, 151, 211.
12. Barnes, A.; Despotakis, A.; Wright, P. V.; Wong, T. C. P.; Chambers, B.; Anderson, A. P. Electron Lett 1996, 32, 358.
13. Wycisk, R.; Pozniak, R.; Pasternak, A. J Electrostat 2002, 56, 55.
14. Pant, R. P.; Dhawan, S. K.; Suri, D. K.; Arora, M.; Gupta, S. K.; Koneracka, M.; Kopcansky, P.; Timko, M. Ind J Eng Mater Sci 2004, 11, 267.
15. Bloom, P. W. M.; Vissenberg, M. C. J. M.; Hulberts, J. N.; Martens, H. C. F.; Schoo, H. F. M. Appl Phys Lett 2000, 77, 2057.
16. Kumar, L.; Dhawan, S. K.; Kamalsannan, M. N.; Chandra, S. Thin Solid Films 2003, 441, 243.
17. Guatafson, G.; Cao, Y.; Treacy, G. M.; Klavetter, F.; Colaneri, N.; Heeger, A. J. Nature 1992, 357, 477.
18. Verma, A.; Sexena, K.; Chanderkant, S.; Dhawan, S. K.; Sharma, R. K.; Sharma, C. P.; Kamalasannan, M. N.; Chandra, S. J Biochem Biotechnol 2001, 96, 215.
19. Jain, S. C.; Aernout, T.; Kapoor, A. K.; Kumar, V.; Geens, W.; Poortmans, J.; Mertens, R. Synth Met 2005, 148, 245.
20. Ishikawa, T.; Nakamura, M.; Fujita, K.; Tsutsui, T. Appl Phys Lett 2003, 84, 2424.
21. Drelinkiewicz, A.; Hasik, M.; Kloc, M. J Catal 1999, 186, 123.
22. Rimbu, G. A.; Jackson, C. L.; Scott, K. J Optoelect Adv Mater 2006, 8, 611.
23. Ding, Y.; Padias, A. B.; Hall, H. K., Jr. J Polym Sci Part A: Polym Chem 1999, 37, 2569.

24. Genies, E. M.; Boyle, A.; Lapkowski, M.; Tsintavis, C. Synth Met 1990, 36, 139.
25. Yu, L. T.; Borredon, M. S.; Josefowicz, M.; Belorgey, G.; Buvet, R. J Polym Sci Polym Symp 1967, 10, 2931.
26. Stafström, S.; Brédas, J. L.; Epstein, A. J.; Woo, H. S.; Tanner, D. B.; Huang, W. S.; MacDiarmid, A. G. Phys Rev Lett 1987, 59, 1464.
27. Dao, L. H.; Leclerc, M.; Guay, J.; Chevalier, J. W. Synth Met 1989, 29, 377.
28. Leclerc, M. J Electroanal Chem 1990, 296, 93.
29. Mattosso, L. H. C.; Faria, R. M.; Bulhoes, L. O. S.; MacDiarmid, A. G.; Epstein, A. J. J. Polym Sci Part A: Polym Chem 1994, 32, 2147.
30. Umare, S. S.; Borkar, A. D.; Gupta, M. C. Bull Mater Sci 2002, 25, 235.
31. Savitha, P.; Rao, P.; Swapna; Sathyanarayana, D. N. Polym Int 2005, 54, 1243.
32. Cao, Y.; Smith, P.; Heeger, A. J. Synth Met 1992, 48, 91.
33. Heeger, A. J. TRIP 1995, 3, 39.
34. Mott, N. F.; Davis, E. A. Electronic Processes in Non-Crystalline Materials, 1st ed.; Clarendon Press: Oxford, 1971.
35. Mott, N. F. Metal–Insulator Transition, 2nd ed.; Taylor & Francis: New York, 1990.
36. Wang, Z. H.; Javadi, H. H. S.; Ray, A.; MacDiarmid, A. G.; Epstein, A. J Phys Rev B 1990, 42, 5411.
37. Li, J.; Fang, K.; Qiu, H.; Li, S.; Mao, W. Synth Met 2004, 142, 107.
38. Reghu, M.; Cao, Y.; Moses, D.; Heeger, A. J Phys Rev B 1993, 47, 1758.
39. Pinto, N. J.; Shah, P. D.; Kahol, P. K.; McCormick, B. J Phys Rev B 1996, 53, 10690.
40. de Albuquerque, J. E.; Mattoso, L. H. C.; Faria, R. M.; Masters, J. G.; MacDiarmid, A. G. Synth Met 2004, 146, 1.
41. Xia, H.; Wang, Q. J Nanopart Res 2001, 3, 401.
42. Asturias, G. E.; MacDiarmid, A. G.; McCall, R. P.; Epstein, A. J. Synth Met 1989, 29, 157.
43. Moon, Y. B.; Cao, Y.; Smith, P.; Heeger, A. J Polym Commun 1989, 30, 196.
44. Pouget, J. P.; Hsu, C. H.; MacDiarmid, A. G.; Epstein, A. J. Synth Met 1995, 69, 11.
45. Cullity, B. D. Elements of X-ray Diffraction, 2nd ed.; Addison-Wesley: London, 1959.
46. MacDiarmid, A. G.; Chiang, J. C.; Richter, A. F.; Epstein, A. J. Synth Met 1987, 18, 285.